

Figure S1. TIRR loss increases 53BP1-dependent gene transactivation property of p53, Related to Figure 1

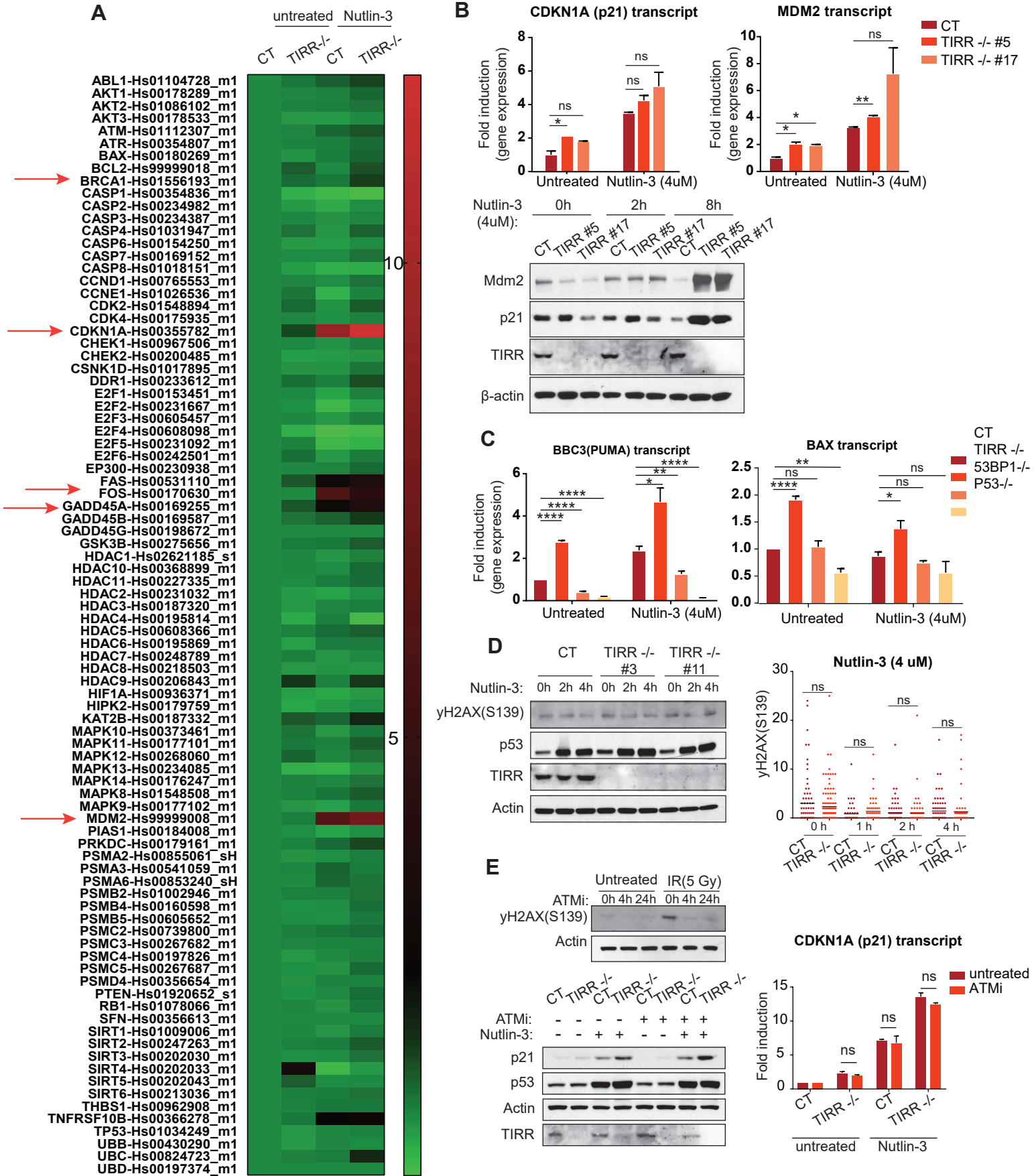


Figure S2. TIRR alters p53-mediated cell fate programs by inhibiting the p53-53BP1 interaction, Related to Figure 3

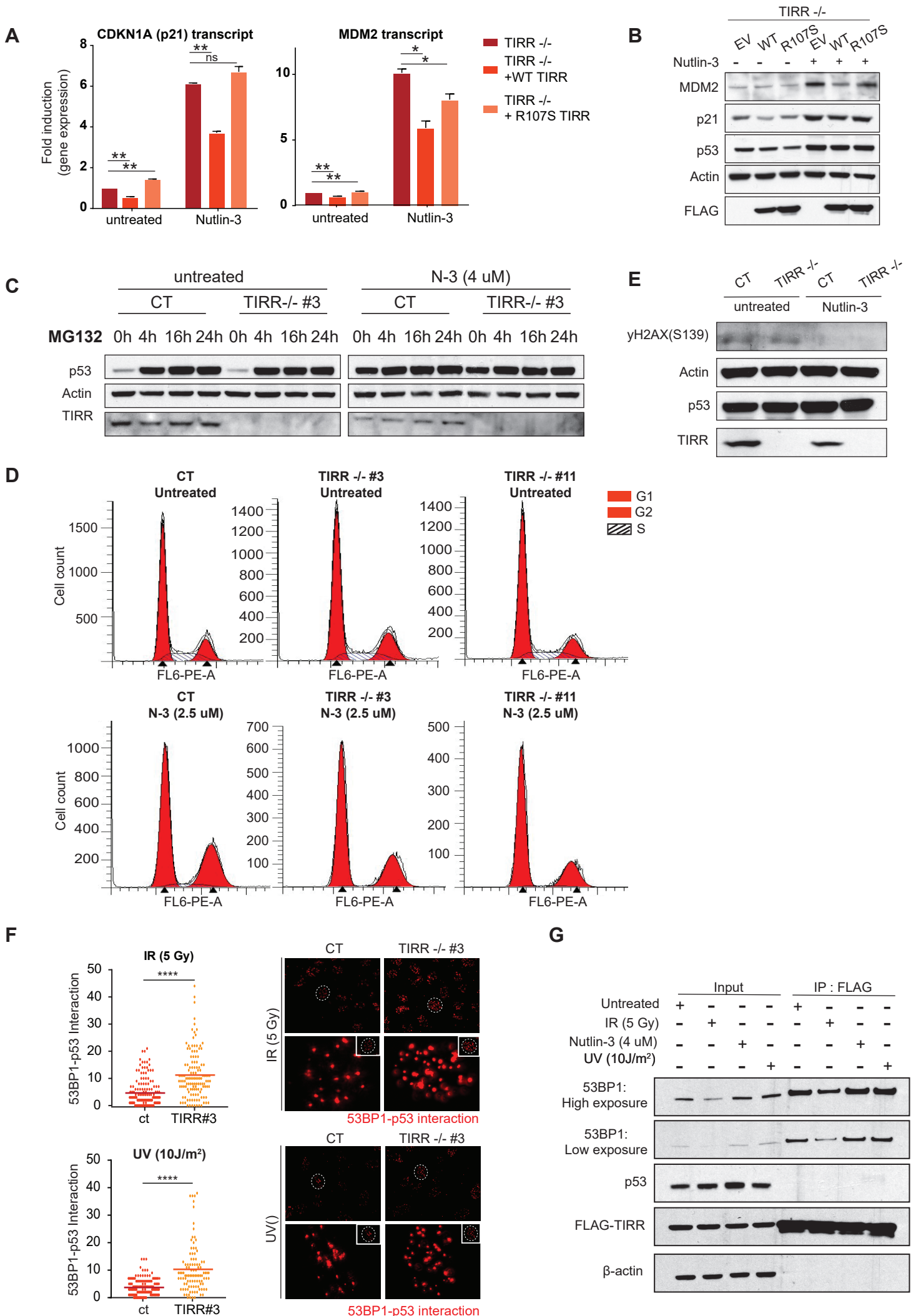


Figure S3. TIRR inhibits the interaction of methylated p53 with the Tudor domain of 53BP1, Related to Figure 4

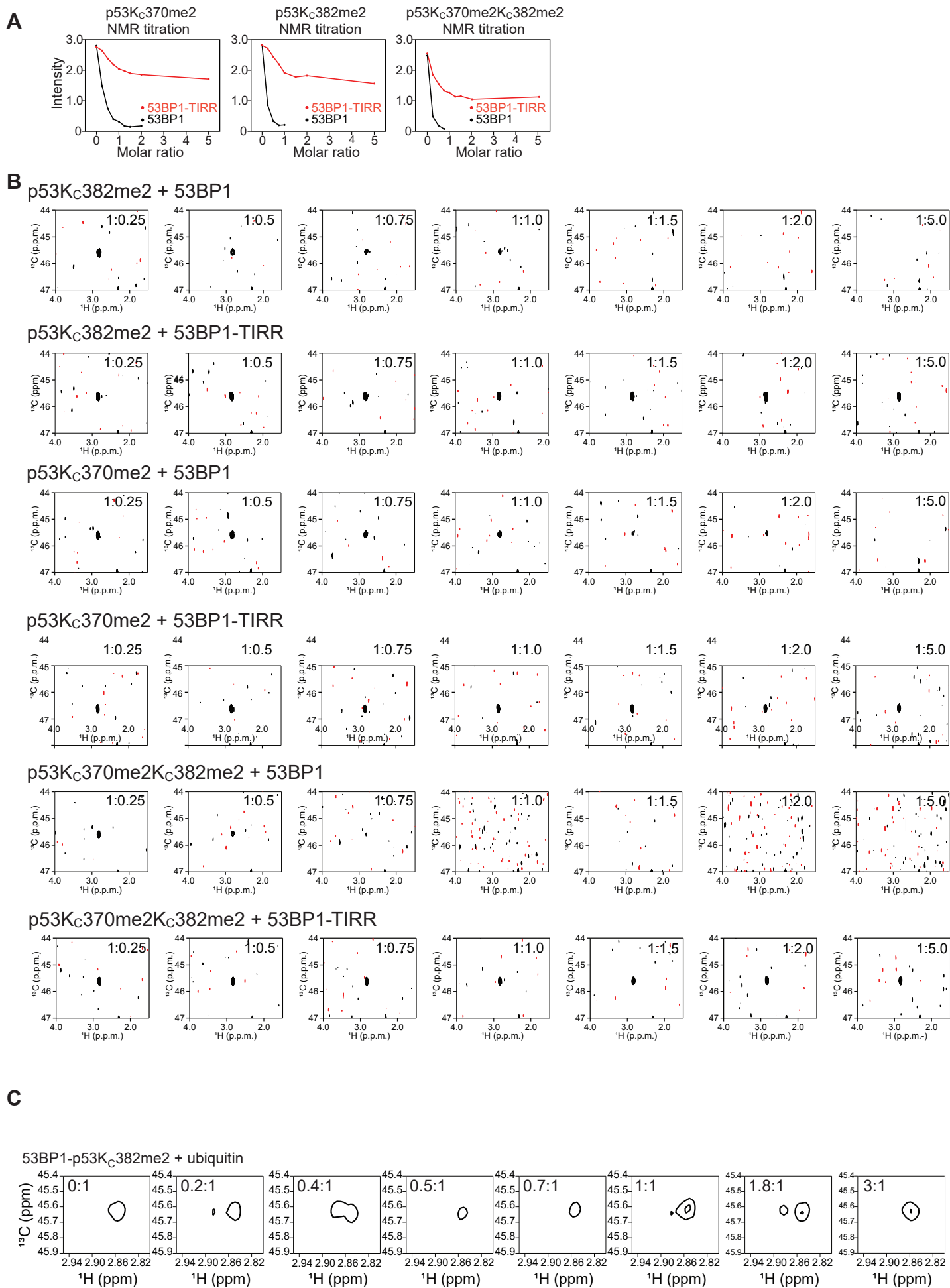


Figure S4. TIRR inhibits the interaction of methylated p53 with the Tudor domain of 53BP1, Related to Figure 4, Figure 5

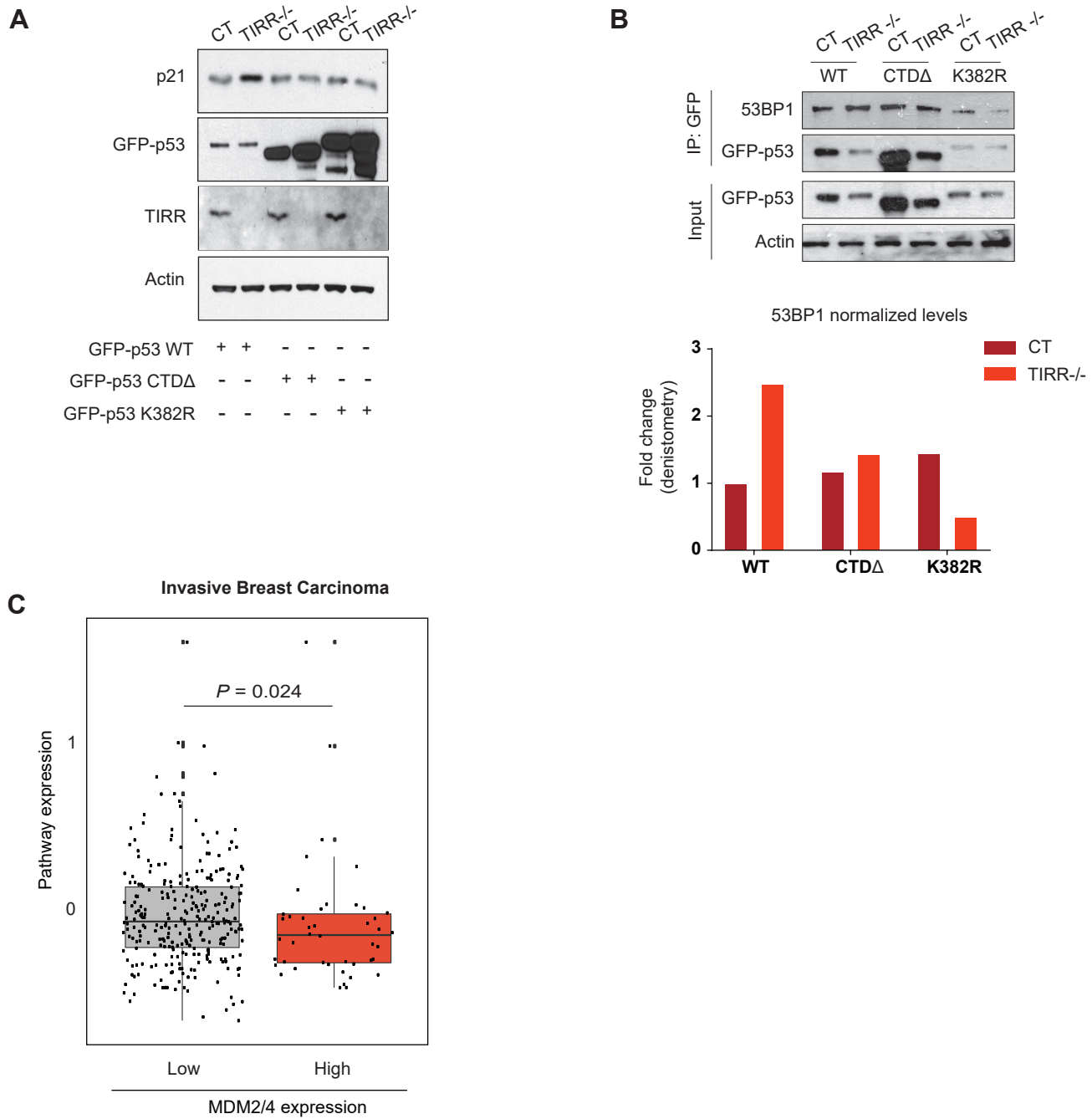


Table S1, Oligonucleotides, Related to STAR Methods

Oligonucleotides	Source	Identifier
p21 F-GGACCTGTCACTGTCTTGTA	IDT	N/A
p21 R- GGCTTCCTCTTGGAGAAGAT	IDT	N/A
MDM2 F-CGTGCCAAGCTTCTCTGTGA	IDT	N/A
MDM2 R-GTCCGATGATTCCTGCTGAT	IDT	N/A
BBC3 F-CTGGAGGGTCCTGTACAATCT	IDT	N/A
BBC3 R-CACCTAATTGGGCTCCATCT	IDT	N/A
BAX F- TTTTCTACTTTGCCAGCAAAC	IDT	N/A
BAX R- GAGGCCGTCCCAACCAC	IDT	N/A
P21-2283 F-AGCAGGCTGTGGCTCTGATT	IDT	N/A
P21-2283 R-AAAATAGCCACCAGCCTCTTCT	IDT	N/A
P21-1391 F-CTGTCCTCCCCGAGGTCA;	IDT	N/A
P21-1391 R- CATCTCAGGCTGCTCAGAGTCT	IDT	N/A
MDM2-5' F-GGCTATTTAAACCATGCATTTTC	IDT	N/A
MDM2-5' R- GTCCGTGCCACAGGTCTA	IDT	N/A

MDM2-3' F-CTTTCTCGAGGAGGCAGGTTT;	IDT	N/A
MDM2-3' R- GCTCAACCCTAGGCGCTATTC	IDT	N/A
ANKRD1 F- AGTAGAGGAACTGGTCACTGG;	IDT	N/A
ANKRD1 R- TGGGCTAGAAGTGTCTTCAGAT	IDT	N/A
EDN1 F- CAGCAGTCTTAGGCGCTGAG	IDT	N/A
EDN1 R- ACTCTTTATCCATCAGGGACGAG	IDT	N/A
IL6 F-CCGGGAACGAAAGAGAAGCT	IDT	N/A
IL6 R- GCGCTTGTGGAGAAGGAGTT	IDT	N/A

Supplementary Figure legends:

Figure S1. TIRR loss increases 53BP1-dependent gene transactivation property of p53, Related to Figure 1.

S1A) Heatmap depicting fold changes in mRNA transcripts of a 92 gene panel that comprised of p53 pathway activators and transcriptional targets, and 4 housekeeping genes. RNA was extracted from RPE1 CT and TIRR-KO cells that were either untreated or treated with Nutlin3, and the corresponding cDNA was analyzed using TaqMan p53 signaling array (See Methods).

S1B) The bar graphs show *p21* and *MDM2* transcript abundance calculated by qRT-PCR in U2OS cells of indicated genotype that were either untreated or treated with Nutlin-3 (4 μ M, 4 hours). The western blot shows the corresponding p21 and MDM2 protein levels in the same cells treated with Nutlin-3 at two different time points. (p-value < 0.0001 (****), p-value = 0.0002-0.0001 (***) , p-value = 0.002-0.0002(**), p-value = 0.0332-0.002 (*), p-value= 0.1234 (ns))

S1C) *BAX* and *BBC3* transcript abundance measured by qRT-PCR in RPE1 cells of indicated genotype that were untreated or treated with Nutlin-3. Mean \pm SD.

S1D) Western blot shows the protein levels of γ H2AX (S139), a DNA damage biomarker, in RPE1 cells of indicated genotype at different timepoints after addition of Nutlin-3; Quantification of γ H2AX(S139) foci by immunofluorescence in RPE1 cells of indicated genotype at different timepoints after treatment with Nutlin-3.

S1E) Western blot shows the protein levels of γ H2AX in RPE1 cells that were either untreated or treated with ATM inhibitor (KU 55933). ATM inhibition reduces the γ H2AX levels in these

cells after 4 hours or even 24 hours of treatment with the inhibitor. The following western blot and bar graph indicate p21 protein and RNA levels in RPE1 CT and TIRR-KO cells that were first either untreated or treated with ATM inhibitor for 24 hours, and then further untreated or treated with Nutlin-3 for 4 hours.

S1F) The bar graphs depict *p21* and *MDM2* transcript abundance calculated by qRT-PCR in RPE1 cells of indicated genotype that were untreated or treated with Nutlin-3. The cells were either untransfected or transfected with an siRNA against USP28. The western blot shows the corresponding p21 and MDM2 protein levels in the same cells.

Figure S2. TIRR alters p53-mediated cell fate programs by inhibiting the p53-53BP1 interaction, Related to Figure 3.

S2A) The bar graphs depict *p21* and *MDM2* transcript abundance calculated by qRT-PCR in RPE1 cells of indicated genotype that were either untreated or treated with Nutlin-3.

S2B) Western blot corresponding to the data shown in Figure S2A.

S2C) Western blot showing p53 protein levels at different timepoints after treatment with MG132 in untreated and Nutlin-3 treated RPE1 CT and TIRR-KO cells.

S2D) Histograms representing the cell cycle profiles corresponding to Fig. 3G.

S2E) Western blot shows to show γ H2AX protein levels in cells represented in Fig. 3G.

S2F) Representative images and quantification of PLA showing endogenous 53BP1-p53 interaction in IR and UV-treated RPE1 CT and TIRR-KO cells.

S2G) FLAG-TIRR interaction complex was extracted by immunoprecipitation in RPE1 TIRR-KO cells stably transduced with FLAG-TIRR. Cells were untreated or treated with either IR (5 Gy) for 90 minutes, or 4 μ M Nutlin-3 for 4 hours, or 10J/m² UV for 2 hours. Indicated proteins were probed in the interacting complex by immunoblotting.

Figure S3. TIRR inhibits the interaction of methylated p53 with the Tudor domain of 53BP1, Related to Figure 4.

S3A) Interaction of methylated p53 with 53BP1 and 53BP1-TIRR probed using NMR spectroscopy. p53 peptides (363-389) ¹³C-dimethylated at lysine analog residues 370 (p53K_C370me₂), 382 (p53K_C382me₂) or 370 and 382 (p53K_C370me₂K_C382me₂) were titrated with 53BP1-Tudor and a preformed 53BP1-Tudor-TIRR complex. Interactions were probed by monitoring the decrease in ¹H-¹³C signal intensity. For straightforward comparison, the molar ratios were reported with respect to the concentration in dimethyllysine analog.

S3B) Shown are the changes in ¹H-¹³C correlation NMR signals of p53K_C370me₂, p53K_C382me₂ and p53K_C370me₂K_C382me₂ (harboring ¹³C-labeled dimethylated lysine analogs) upon titration with 53BP1-Tudor or 53BP1-Tudor-TIRR. The peptide:protein ratios are indicated. These signals were integrated to generate Fig. S3A.

S3C) Positive control for Fig. 4A. Ubiquitin, which does not bind 53BP1, has no effect on the 53BP1-Tudor-p53K_C382me₂ interaction.

Figure S4. TIRR inhibits the interaction of methylated p53 with the Tudor domain of 53BP1, Related to Figure 4, Figure 5.

S4A) p21 protein levels assessed by western blot in RPE1 CT and TIRR-KO cells that were transfected with either WT p53, or the C-terminal deleted mutant (CTD Δ) or the K382R mutant.

S4B) GFP-p53 was immunoprecipitated from RPE1 CT and TIRR-KO cells expressing either WT p53, or the C-terminal deleted mutant (CTD Δ) or the K382R mutant. 53BP1 levels in the interacting complex were analyzed by immunoblotting. The bar graph shows the normalized amounts of 53BP1 in the immunoprecipitated fraction.

S4C) Positive control for Fig. 5C. Pathway expression in invasive breast carcinoma (left) with and without MDM2 amplification. Pathway expression scores were calculated as the average mRNA expression of p53 pathway members. RNAseq data for each p53 pathway gene were obtained from TCGA and were evaluated as z-scores relative to diploid samples. P-values, Wilcoxon test.